Chapter 5

Coupled Kicked Top

5.1 Introduction

We discussed in Chapter 3 that the single kicked top is a well studied system whose classical dynamics displays chaos and its quantum spectrum follows the standard threefold statistics of Wigner-Dyson. Two such single kicked tops coupled by an interaction was studied in the context of establishing the relation between classical chaos and quantum entanglement [69, 111, 112]. Here, from the Floquet perspective, the coupled kicked top (CKT) system is interesting because, it is classically a higher-dimensional system (four dimension) and hence its effective Hamiltonian is expected to be nonintegrable. Earlier studies, including the result discussed in Chapter 3, of lower dimensional nonintegrable systems showed that the effective Hamiltonian is integrable [54]. Here we derive the effective Hamiltonian of the CKT perturbatively by both Van Vleck and Brillouin-Wigner schemes at very large frequency limit. We study the effective Hamiltonian both classically and quantum mechanically. The classical dynamics of this system shows chaos and its quantum spectrum follows interesting nonstandard symmetry classes or nonstandard statistics [72, 73]. This classes are based on Cartan's tenfold classification of symmetry

spaces [113].

In the following section, i.e., Sec. 5.2, we introduce the couple kicked top model. Then in Sec. 5.3, we study this system from Floquet theory perspective and derived the effective Hamiltonian from Van Vleck and Brillouin-Wigner expansion. In Sec. 5.4, we present the classical dynamics of the effective Hamiltonian. Section 5.5 discusses quantum mechanical properties of the system described by the effective Hamiltonian. Finally, we conclude this chapter in Sec. 5.6

5.2 Model

We consider a coupled kicked top system whose Hamiltonian is given as:

$$H(t) = H_1(t) \otimes \mathbb{1} + \mathbb{1} \otimes H_2(t) \; + \; H_{12}(t), \tag{5.1}$$

where

$$H_i(t) = \frac{p_i}{T} J_{xi} \; + \; \frac{k_i}{2j} J_{zi}^2 \sum_n \delta(t-n), \tag{5.2}$$

and

$$H_{12}(t) = \frac{\epsilon}{j} J_{z1} \otimes J_{z2} \sum_n \delta(t-n). \tag{5.3}$$

The first two terms are representing the Hamiltonian of the individual top and the third term is the coupling between the tops. This Hamiltonian is represented by the angular momentum operators $\mathbf{J} = (J_{xi}, J_{yi}, J_{zi})$ which follow usual angular momentum algebra $[J_{\alpha i}, J_{\beta i}] = \imath\, \varepsilon_{\alpha\beta\gamma,i}\, J_{\gamma i}$ and $i = 1, 2$ are denoting individual top. Here, $\imath = \sqrt{-1}$ and the standard Levi-Civita symbol ε is introduced to indicate the cyclic permutation in the commutator relations. The angular momentum operators of the different tops commute, i.e., $[J_{\alpha 1}, J_{\beta 2}] = 0$ for all $\alpha, \beta \in (x, y, z)$. The first term in the Hamiltonian of individual top describes the free precession of the top

around x-axis with angular velocity p_i/T, and the second term describes torsion about z-axis by an angle proportional to J_{zi} where the proportionality constant k_i is a dimensionless quantity. The second term is acting on the individual top in δ-kicked fashion. These two tops are also interacting in δ-kicked fashion and ϵ is the coupling strength between them. Therefore, the total Hamiltonian is:

$$\begin{aligned} H(t) = & \frac{1}{T}\left(p_1 J_{x1}\otimes\mathbb{1} + p_2\mathbb{1}\otimes J_{x2}\right) \\ & + \frac{1}{2j}\left(k_1 J_{z1}^2\otimes\mathbb{1} + k_2\mathbb{1}\otimes J_{z2}^2 + 2\epsilon J_{z1}\otimes J_{z2}\right)\sum_n \delta(t-nT). \end{aligned} \tag{5.4}$$

Corresponding Floquet operator, or the time-evolution operator between two consecutive kicks, is:

$$U(T) = e^{-\imath\frac{\epsilon}{jT}J_{z1}\otimes J_{z2}}\left[e^{-\imath\frac{k_1}{2jT}J_{z1}^2\otimes\mathbb{1}}\, e^{-\imath p_1 J_{x1}\otimes\mathbb{1}} \otimes e^{-\imath\frac{k_2}{2jT}\mathbb{1}\otimes J_{z2}^2}\, e^{-\imath p_2\mathbb{1}\otimes J_{x2}}\right]. \tag{5.5}$$

5.3 The effective Hamiltonian of the CKT system

We now derive the effective Hamiltonian of the CKT system using both Van Vleck and Brillouin-Wigner perturbation theories. The general expression of the effective Hamiltonian up to $\mathcal{O}(\omega^{-2})$ for the δ-kicked case has already been derived in Eqs. (2.29) and (2.42) of Chapter 2. We rewriting the same expression here for the sake of completeness:

$$\begin{aligned} H_{\mathrm{VV}} &= H_0 + \frac{V}{T} + \frac{1}{24}\left[\left[V, H_0\right], V\right] = H_0 + \frac{V}{T} + \frac{1}{12}VH_0V - \frac{1}{24}\left(H_0V^2 + V^2H_0\right) \\ \text{and} \\ H_{\mathrm{BW}} &= H_0 + \frac{V}{T} + \frac{1}{12}VH_0V. \end{aligned} \tag{5.6}$$

The above two expressions are identical at the ω^0 order; but $H_{\rm VV}$ has two additional terms at ω^{-2} order. We have already discussed in Chapter 2 that, at the infinite order of accuracy, the effective Hamiltonian corresponding to different perturbation theories are connected by some gauge transformation. However, when we truncate the expansion at a certain finite order, then the gauge connection between different Hamiltonians is lost. Here we are witnessing this situation. In the above effective Hamiltonians, the third term has come from ω^{-2} order, and we substitute $\omega T = 2\pi$ to get the ω independent term. The presence of the factor $1/12$ (or $1/24$) is reducing the effect of this second order term on the classical dynamics and also on the quantum spectrum very much. Our numerics also prove this fact. Therefore, in order to simplify the analysis, we are ignoring the second order term. Now the effective Hamiltonians obtained from two different perturbation theories are identical, i.e.,

$$\begin{aligned} H_{\rm eff} &= H_0 + \frac{V}{T} \\ &= \frac{1}{T}\left[\left(p_1 J_{x1}\otimes\mathbb{1} + p_2\mathbb{1}\otimes J_{x2}\right) + \frac{1}{2j}\left(k_1 J_{z1}^2\otimes\mathbb{1} + k_2\mathbb{1}\otimes J_{z2}^2 + 2\epsilon J_{z1}\otimes J_{z2}\right)\right] \end{aligned} \tag{5.7}$$

According to the definition given in the original Hamiltonian, the parameters p_is are the total rotation angle, k_is are the total torsional angle, and ϵ total coupling within the time interval T. We now rescaling these parameters as $\Omega_i = p_i/T$, $\kappa_i = k_i/T$, and $\tilde{\epsilon} = \epsilon/T$, where Ω_is are the angular rotation rate or angular velocity, κ_is are the torsional rate, and $\bar{\epsilon}$ rate of coupling. Therefore, in terms of the rescaled parameters, the effective Hamiltonian becomes

$$H_{\rm eff} = \left(\Omega_1 J_{x1} + \Omega_2 J_{x2}\right) + \frac{1}{2j}\left(\kappa_1 J_{z1}^2 + \kappa_2 J_{z2}^2 + 2\,\tilde{\epsilon} J_{z1} J_{z2}\right). \tag{5.8}$$

Here we have dropped all the tensor product notations $\otimes$. The suffices $i = 1, 2$ are denoting the individual Hilbert space of the two tops, and thus indicating the underlying tensor product structure of the two Hilbert spaces.

5.4 Classical dynamics of the effective Hamiltonian of the CKT

The classical dynamics of the angular momentum operators dependent quantum Hamiltonian can be defined in various ways. One method is to consider the quantum Hamiltonian as a classical Hamiltonian and replace all the commutator brackets of the angular momentum operators by the generalized Poisson brackets introduced by Martin [114]. Then derive the equation of motion for all the "components" of angular momentum using the generalized Poisson brackets. However, there is an equivalent method by which we can also derived the equation of motion. First, we write down the Heisenberg's equation of motion for all the components of the angular momentum operators, i.e. $\frac{dJ_{\alpha i}}{dt} = -\imath\,[J_{\alpha i}, H_{\text{eff}}]$, then divide the both sides by the spin j, identify the rescaled angular momentum operators $J_{\alpha i}/j$, and take the classical limit $j \to \infty$. The rescaled angular momentum operators at $j \to \infty$ limit become classical variables and commute with each other. For example: $J_x/j \to X$ and $J_y/j \to Y$, then $[X, Y] = \imath Z/j$ where $J_z/j \to Z$; then at $j \to \infty$ limit, the right hand side of the commutator bracket relation will be zero. The rescaled angular momentum variables satisfy the constraint $X_1^2 + Y_1^2 + Z_1^2 = X_2^2 + Y_2^2 + Z_2^2 = 1$. This means that the classical dynamics of the coupled top takes place on the surface of 2-spheres. The straightforwardness of the later method, prompts us to apply it to derive the classical equation of motion.

Following the above prescription, we are illustrating rigorous derivation of the

equation of motion of only one component of the angular momentum, say J_{x1}. Others are derived identically, and we just present the final form of them. Equation of motion of angular momentum operator J_{x1} can be obtained as:

$$\begin{aligned}\frac{dJ_{x1}}{dt} &= -\imath[J_{x1}, H_{\text{eff}}] \\ &= -\frac{\imath}{2j}\left(\kappa_1\,[J_{x1}, J_{z1}^2] + 2\tilde{\epsilon}\,[J_{x1}, J_{z1}]J_{z2}\right) \\ &= -\frac{\imath}{2j}\Big\{\kappa_1\left([J_{x1}, J_{z1}]J_{z1} + J_{z1}[J_{x1}, J_{z1}]\right) + 2\tilde{\epsilon}\,[J_{x1}, J_{z1}]\,J_{z2}\Big\} \\ &= -\frac{1}{2j}\Big(\kappa_1\big(J_{y1}J_{z1} + J_{z1}J_{y1}\big) + 2\tilde{\epsilon}\,J_{y1}J_{z2}\Big).\end{aligned} \tag{5.9}$$

Now, dividing the above equation with j and obtain the form:

$$\frac{1}{j}\frac{dJ_{x1}}{dt} = -\frac{\kappa_1}{2}\left(\frac{J_{y1}}{j}\frac{J_{z1}}{j} + \frac{J_{z1}}{j}\frac{J_{y1}}{j}\right) - \tilde{\epsilon}\,\frac{J_{y1}}{j}\frac{J_{z2}}{j}. \tag{5.10}$$

We now set $j \to \infty$ limit, and get the classical equation of motion as:

$$\frac{dX_1}{dt} = -Y_1\big(\kappa_1\,Z_1 + \tilde{\epsilon}\,Z_2\big). \tag{5.11}$$

Following the above steps, we obtain the full equation of motion as:

$$\begin{aligned}\dot{X}_1 &= -Y_1\big(\kappa_1\,Z_1 + \tilde{\epsilon}\,Z_2\big), \\ \dot{Y}_1 &= -\Omega_1\,Z_1 + X_1\big(\kappa_1\,Z_1 + \tilde{\epsilon}\,Z_2\big), \\ \dot{Z}_1 &= \Omega_1\,Y_1, \\ \dot{X}_2 &= -Y_2\big(\kappa_2\,Z_2 + \tilde{\epsilon}\,Z_1\big), \\ \dot{Y}_2 &= -\Omega_2\,Z_2 + X_2\big(\kappa_2\,Z_2 + \tilde{\epsilon}\,Z_1\big), \\ \dot{Z}_2 &= \Omega_2\,Y_2.\end{aligned} \tag{5.12}$$

We mentioned earlier that the above equation of motion can also be obtained by

Martin's generalized Poisson bracket. For this, we also have to identify the classical effective Hamiltonian in terms of the rescaled angular momenta as:

$$H^{\rm cl} = \lim_{j\to\infty} \frac{H_{\rm eff}}{j} = \left(\Omega_1\, X_1 + \frac{1}{2}\kappa_1\, Z_1^2\right) + \left(\Omega_2\, X_2 + \frac{1}{2}\kappa_2\, Z_2^2\right) + \tilde{\epsilon}\, Z_1 Z_2. \qquad (5.13)$$

We can exploit the constraints $X_1^2 + Y_1^2 + Z_1^2 = X_2^2 + Y_2^2 + Z_2^2 = 1$ to reduce the degrees of freedom *six* to *four*. For that, we parameterize the angular momentum variables as $X_i = \sin\theta_i \cos\phi_i$, $Y_i = \sin\theta_i \sin\phi_i$, and $Z_i = \cos\theta_i$, where Z_i and ϕ_i become canonically conjugate variables for the i-th top. In terms of this new parameterization, the classical Hamiltonian becomes

$$H^{\rm cl} = \Omega_1 \sqrt{1 - Z_1^2}\, \cos\phi_1 + \Omega_2 \sqrt{1 - Z_2^2}\, \cos\phi_2 + \frac{1}{2}\big(\kappa_1 Z_1^2 + \kappa_2 Z_2^2\big) + \tilde{\epsilon}\, Z_1 Z_2. \quad (5.14)$$

and the corresponding Hamiltonian's equations of motion are derived as:

$$\begin{aligned}
\dot{Z}_1 &= -\frac{\partial H^{\rm cl}}{\partial \phi_1} = \Omega_1 \sqrt{1 - Z_1^2}\, \sin\phi_1 \\
\dot{\phi}_1 &= \frac{\partial H^{\rm cl}}{\partial Z_1} = \kappa_1\, Z_1 - \frac{\Omega_1 Z_1}{\sqrt{1 - Z_1^2}} \cos\phi_1 + \tilde{\epsilon}\, Z_2, \\
\dot{Z}_2 &= -\frac{\partial H^{\rm cl}}{\partial \phi_2} = \Omega_2 \sqrt{1 - Z_2^2}\, \sin\phi_2 \\
\dot{\phi}_2 &= \frac{\partial H^{\rm cl}}{\partial Z_2} = \kappa_2\, Z_2 - \frac{\Omega_2 Z_2}{\sqrt{1 - Z_2^2}} \cos\phi_2 + \tilde{\epsilon}\, Z_1.
\end{aligned} \qquad (5.15)$$

Here, exploiting the two constraints, we have reduced the number of equations of motion from *six* to *four*.

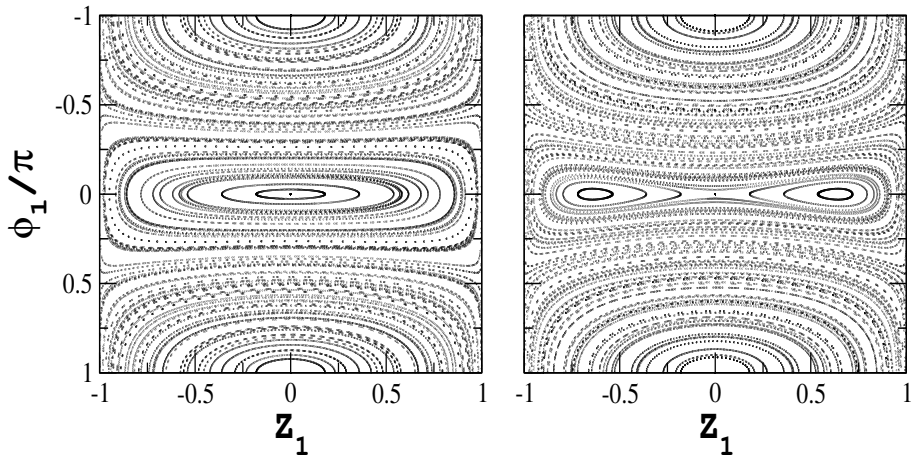

FIGURE 5.1: The dynamics of the coupled top is projected on the phase space of the first top at the FP limit. The FP limit is obtained by setting $\kappa_1 = \kappa_2 = 0$. We set $\Omega_1 = \Omega_2 = 1.0$. Left panel: Coupling $\tilde{\epsilon} = 0.8$; and Right panel: $\tilde{\epsilon} = 1.3$.

5.4.1 Feingold-Peres (FP) limit

The Feingold-Peres (FP) Hamiltonian is an autonomous model of coupled top system. The presence of nonlinear angular momentum terms in our H_{eff} of the coupled kicked top makes it different from the FP Hamiltonian. Therefore, by setting $\kappa_1 = \kappa_2 = 0$, we can get the FP Hamiltonian from H_{eff}. In Fig. 5.1, we present the phase space dynamics of the coupled top at the FP limit. Here, we fix $\Omega_1 = \Omega_2 = 1.0$ and consider two different coupling strengths $\tilde{\epsilon} = 0.8$ (Left panel) and $\tilde{\epsilon} = 1.3$ (Right panel). We have chosen these two coupling strengths, because at $\tilde{\epsilon} = 1.0$, the phase space dynamics of the FP system makes a transition, which is clear from the appearance of substructures at the center.

5.4.2 Nonzero torsions case

We study the dynamics due to the effective Hamiltonian H_{eff} of the couple kicked top in presence of the nonlinear torsions κ_1 and κ_2. Here, again we set the parameters $\Omega_1 = \Omega_2 = 1.0$ and consider the same two coupling cases, $\tilde{\epsilon} = 0.8$ and 1.3, to show the effect of the torsional terms on the dynamics of FP model. In Fig. 5.2,

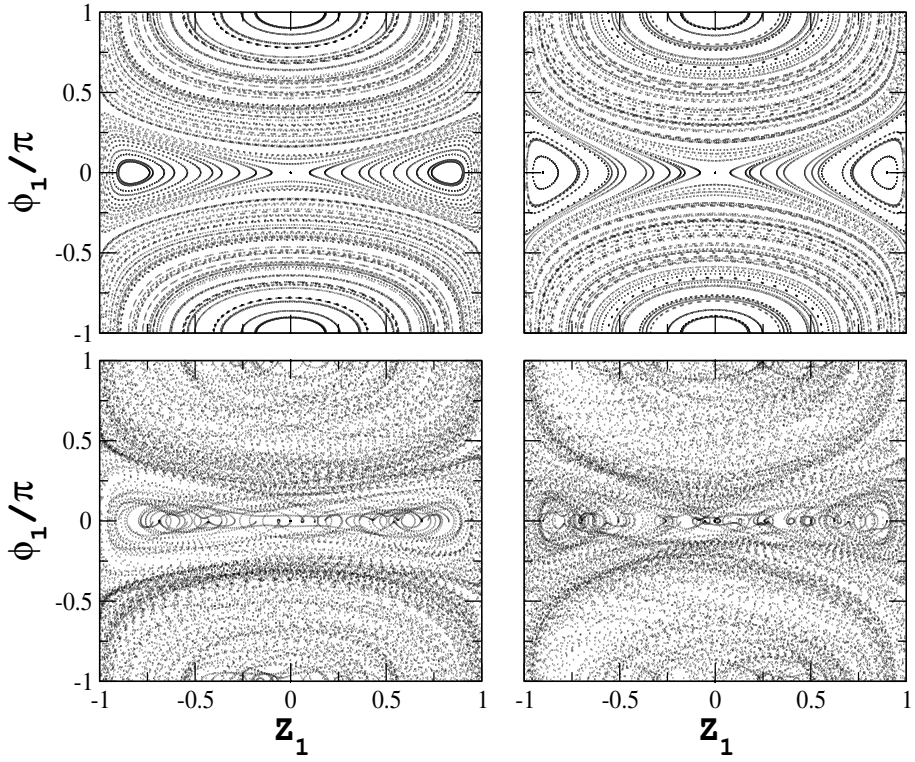

FIGURE 5.2: The dynamics of the coupled top is projected on the phase space of the first top. We again set $\Omega_1 = \Omega_2 = 1.0$ and consider the same coupling strengths. Here, we have considered nonzero values of the torsion parameters κ_1 and κ_2. Top-Left panel: $\tilde{\epsilon} = 0.8$ and $\kappa_1 = \kappa_2 = 1.0$; Top-Right panel: $\tilde{\epsilon} = 1.3$ and $\kappa_1 = \kappa_2 = 1.0$; Bottom-Left panel: $\tilde{\epsilon} = 0.8$ and $\kappa_1 = -\kappa_2 = 1.0$; Bottom-Right panel: $\tilde{\epsilon} = 1.3$ and $\kappa_1 = -\kappa_2 = 1.0$. We observe completely different behavior of the phase space dynamics, when we consider κ_1 and κ_2 of the same magnitude but of opposite signs.

we consider two cases of torsions: at the top panels, two torsional terms are equal in magnitude and sign; and at the bottom panels, we consider torsional terms with opposite sign, but of the same magnitude. For the first case, presented in the top panels, for both the coupling strengths the dynamics is qualitatively similar. This behavior is completely different than the FP case, as discussed above. However, for the later case, when the torsions are of the opposite sign, the dynamics is very much different from the case having torsions with same sign. Here, we see at the center part of the phase space of the first top, the trajectories are going from one stable island to another. The point is to note that we have not plotted the Poincare section; instead, we have just projected the phase space trajectories of the CKT

residing on the four-dimensional phase space to the phase space of the first top having dimension two. Therefore, these flow of trajectories from one island to another is actually happening through higher dimensional phase space. We can also see such flow of trajectories from one region to another at the other parts of the phase space.

5.5 Symmetry properties of the effective Hamiltonian of the CKT

5.5.1 Feingold-Peres (FP) limit

At the FP limit, the effective Hamiltonian of the CKT becomes

$$H_{\text{eff}} = H_{\text{FP}} = \Omega_1 J_{x1} + \Omega_2 J_{x2} + \frac{\tilde{\epsilon}}{j} J_{z1} J_{z2}. \tag{5.16}$$

If $\Omega_1 = \Omega_2$, the above Hamiltonian has permutation symmetry, i.e., if we exchange the two tops $1 \leftrightarrow 2$, then the FP Hamiltonian remains invariant. Besides, the above Hamiltonian has a unitary symmetry

$$U_0 = e^{-\imath\pi J_{x1}} \otimes e^{-\imath\pi J_{x2}}, \tag{5.17}$$

such that $U_0\, H_{\text{FP}}\, U_0^\dagger = H_{\text{FP}}$ or $[U_0, H_{\text{FP}}] = 0$, where $U_0^2 = \mathbb{1}$. The FP Hamiltonian has an additional unitary symmetry

$$C = e^{\imath\alpha} e^{-\imath\pi J_{z1}} \otimes e^{-\imath\pi J_{y2}}, \tag{5.18}$$

which gives $C\,H_{\rm FP}\,C^{\dagger} = -H_{\rm FP}$ or $(C\,H_{\rm FP} + H_{\rm FP}\,C) = 0$. This also implies that $\mathrm{Tr}\,(H_{\rm FP}) = 0$. The phase factor $e^{i\alpha}$ is not playing any role here to show this symmetry of $H_{\rm FP}$ under C, because its complex conjugate factor from $C^{\dagger}$ part will trivially cancel it. However, this innocent looking phase factor will become important while classifying the system under different symmetry classes. The operator C is called chirality operator. In case of the integer spin $C^2 = \mathbb{1}$. This property of $H_{\rm FP}$ implies the presence of nonstandard symmetries, which are different from the standard Wigner-Dyson threefold symmetry classes. In addition, the FP Hamiltonian has a nonunitary symmetry like the time-reversal symmetry. We denote the time-reversal operator $\mathcal{T}$, which is in standard basis, flips the sign of J_y operator but keep the other two angular momenta invariant. Therefore, $H_{\rm FP}$ also satisfies $\mathcal{T}\,H_{\rm FP}\mathcal{T}^{-1} = H_{\rm FP}$. Depending on whether the chirality operator C commutes with $\mathcal{T}$, we get different classes of symmetries for $H_{\rm FP}$. If the spin j is integer, then we set $\alpha = 0$ and find that

$$\begin{aligned}
\mathcal{T}\,C\,\mathcal{T}^{-1} &= \mathcal{T}\left[e^{-\imath\pi J_{z1}} \otimes e^{-\imath\pi J_{y2}}\right]\mathcal{T}^{-1} \\
&= e^{\imath\pi J_{z1}} \otimes e^{-\imath\pi J_{y2}} \\
&= e^{2\imath\pi J_{z1}}\, e^{-\imath\pi J_{z1}} \otimes e^{-\imath\pi J_{y2}} \\
&= C,
\end{aligned} \tag{5.19}$$

where we use $\mathcal{T}\,\imath\,\mathcal{T}^{-1} = -\imath$; and for integer j, the term $e^{2\imath\pi J_{z1}}$ becomes identity matrix. Thus we find $\mathcal{T}\,C\,\mathcal{T}^{-1} = C$. However, for the half-integer spin $e^{2\imath\pi J_{z1}} \neq \mathbb{1}$ and hence $\mathcal{T}\,C\,\mathcal{T}^{-1} \neq C$. For this case, the phase α can be tuned to get a C which

commutes with $\mathcal{T}$. For any arbitrary phase α, we have,

$$\begin{aligned}\mathcal{T}\,C\,\mathcal{T}^{-1} &= \mathcal{T}\left[e^{\imath\alpha}e^{-\imath\pi J_{z1}}\otimes e^{-\imath\pi J_{y2}}\right]\mathcal{T}^{-1}\\ &= e^{-\imath\alpha}e^{\imath\pi J_{z1}}\otimes e^{-\imath\pi J_{y2}}\\ &= e^{-\imath 2\alpha}\,e^{\imath 2\pi J_{z1}}\,\left[e^{\imath\alpha}\,e^{-\imath\pi J_{z1}}\,\otimes e^{-\imath\pi J_{y2}}\right]\\ &= e^{\imath 2(\pi J_{z1}-\alpha)}\,C.\end{aligned} \tag{5.20}$$

If we set $\alpha = \pi\, j$, then for both integer and half-integer spin j, the first term of the last equality in the above equation will be an identity operator. Hence, we find that, the chirality operator

$$C = e^{\imath\pi j}e^{-\imath\pi J_{z1}}\otimes e^{-\imath\pi J_{y2}} \tag{5.21}$$

is time reversal symmetric, i.e., $\mathcal{T}\,C\,\mathcal{T}^{-1} = C$ and also transforms the FP Hamiltonian as $C\,H_{\rm FP}\,C^{-1} = -H_{\rm FP}$. We note that for the integer spin j, the chirality operator satisfies $C^2 = \mathbb{1}$; and for the half-integer spin, $C^2 = -\mathbb{1}$. Due to the presence of a time-reversal symmetric chirality operator, the FP limit of the CKT model is classified as: **(i)** the BDI (BD One) class or the chiral orthogonal symmetry class for $C^2 = \mathbb{1}$ (integer spin); and **(ii)** the CI (C One) class or the anti-chiral class for $C^2 = -\mathbb{1}$ (half-integer spin). These are two classes of the so-called non-standard symmetries [73]. This analysis of the FP Hamiltonian is performed on the basis of a recent publication [72].

5.5.2 Nonzero torsions case

In case of the nonzero torsions, consider the case $\kappa_1 = \kappa_2 = \kappa$ and also $\Omega_1 = \Omega_2 = \Omega$. Then the effective Hamiltonian for the CKT, denoted by $H_{\rm CT}$ (CT stands for

coupled top), will be

$$\begin{aligned} H_{\rm CT} &= \Omega\big(J_{x1}+J_{x2}\big) + \frac{\tilde{\epsilon}}{j}J_{z1}J_{z2} + \frac{\kappa}{2j}\left(J_{z1}^2+J_{z2}^2\right) \\ &= H_{\rm FP} + \frac{\kappa}{2j}\left(J_{z1}^2+J_{z2}^2\right) \\ &\equiv H_{\rm FP} + H_{\rm NL}, \end{aligned} \tag{5.22}$$

where $H_{\rm NL}$ is the nonlinear torsion part. This Hamiltonian is clearly symmetric under permutation and it also remains invariant under the unitary transformation U_0 defined earlier. However, this Hamiltonian does not show chiral symmetry under the transformation C, i.e., $CH_{\rm CT}C^\dagger \neq -H_{\rm CT}$. This is simply because $H_{\rm NL}$ does not have chiral symmetry, i.e., $C\,H_{\rm NL}\,C^{-1} \neq -H_{\rm NL}$. This is also the consequence of *nonzero* trace of $H_{\rm NL}$.

We now find the condition for which the trace can be zero. Starting with a different torsion strengths $\kappa_1 \neq \kappa_2$, we calculate the trace in the standard basis as:

$$\begin{aligned} {\rm Tr}\left(H_{\rm NL}\right) &= \frac{1}{2j}\left(\kappa_1\sum_{m_1=-j}^{j} m_1^2 + \kappa_2\sum_{m_2=-j}^{j} m_2^2\right) \\ &= \frac{2}{j}\sum_{m=1}^{j} m^2\left(\kappa_1+\kappa_2\right) \\ &= \frac{1}{3}(j+1)(2j+1)\left(\kappa_1+\kappa_2\right). \end{aligned} \tag{5.23}$$

The above relation clearly shows that, when $\kappa_1 = -\kappa_2 = \kappa$, then the trace will be zero. Therefore, the CT Hamiltonian with trace zero is of the form

$$H_{\rm CT} = \Omega\big(J_{x1}+J_{x2}\big) + \frac{\tilde{\epsilon}}{j}J_{z1}J_{z2} + \frac{\kappa}{2j}\left(J_{z1}^2-J_{z2}^2\right). \tag{5.24}$$

Note that, for this particular case of the torsion with opposite signs, we have seen a very different kind of classical dynamics. However, still the Hamiltonian $H_{\rm CT}$ does not have the chiral symmetry under the transformation of C. This implies that

there exists a different chirality operator, say C', under which $C'\,H_{\rm CT}\,C'^{\dagger} = -H_{\rm CT}$. One point is to be noted that now the Hamiltonian $H_{\rm CT}$ is not symmetric under permutation. We exploit this fact and obtain $C' = PC$, where P is the permutation operator. One can now easily check that $C'\,H_{\rm CT}\,C'^{\dagger} = P\,C\,H_{\rm CT}\,C^{\dagger} = -H_{\rm CT}$ or $(C'\,H_{\rm CT} + H_{\rm CT}\,C') = 0$. Since the chirality operator C is time-reversal symmetric, then trivially one can show that the chirality operator C' for the couple top Hamiltonian is also time-reversal symmetric. Moreover, for $C'^2 = \pm\mathbb{1}$, the other chirality operator also satisfies exactly the same property, i.e., $C'^2 = \pm\mathbb{1}$. Therefore, the CT Hamiltonian can also be classified into two same chiral symmetry classes BDI and CI. Besides, for the nonzero trace case, one can not find a chirality operator under which the CT Hamiltonian will show the symmetry property, therefore this Hamiltonian belongs to the standard symmetry class.

5.6 Conclusion

In this chapter, we have analyzed a coupled kicked top system from the Floquet theory perspective. The effective Hamiltonian obtained from this time dependent system at the *zeroth* order of the perturbation theory (here the first order term is zero) shows nonintegrability. We have shown that, at one particular limit, the effective Hamiltonian becomes the well known Feingold-Peres model. We study the classical dynamics of the effective Hamiltonian at the Feingold-Peres limit as well as for the general case. We have observed that the classical dynamics are qualitatively different for the two cases. At the quantum mechanical level, we study the symmetry properties of the effective Hamiltonian. We find that, for both the cases, the Hamiltonian follows the recently proposed nonstandard symmetry classes BDI or chiral orthogonal symmetry and CI or anti-chiral orthogonal symmetry. Moreover, at the FP limit, the Hamiltonian also has the permutation symmetry.

However, the permutation symmetric coupled top Hamiltonian does not have the chiral symmetry. In order to make it chiral symmetric, we have to break the permutation symmetry. Rather, the breaking of the permutation symmetry actually facilitates to construct a chirality operator for the coupled top Hamiltonian.